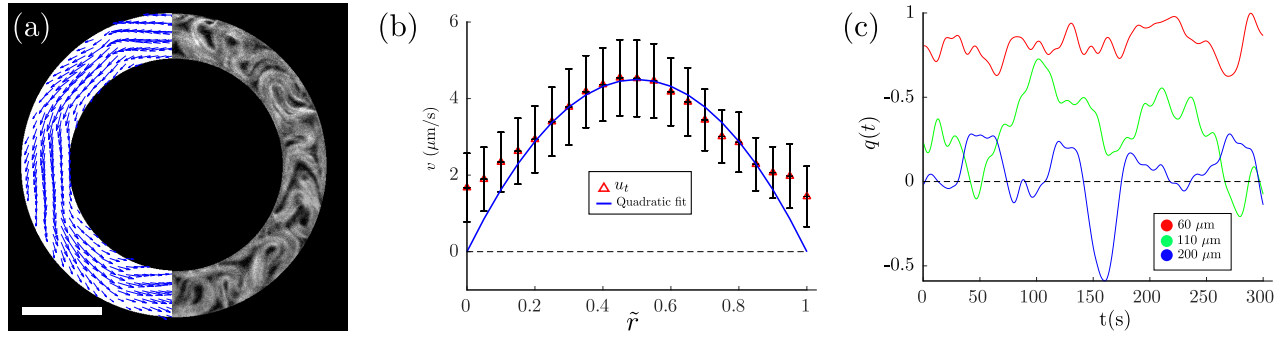


## **Supplementary Information**

### **Active microfluidic transport in two-dimensional handlebodies**

Jérôme Hardoüin, Justine Laurent, Teresa Lopez-Leon, J. Ignés-Mullol and Francesc Sagués

## **Supplementary Figures**



**Fig. S1 Particle Image Velocimetry of active flows confined in annuli.** (a) Fluorescence micrograph of an active nematic confined in a  $60\ \mu\text{m}$  annulus, with the corresponding velocity field overlaid in blue. The velocity field is averaged over 600 frames at 2 frames per second. The image is overlapped with a black mask around the region of interest, for a better visualization. (b) Tangential velocity  $u_t$  fitted with a Poiseuille-like velocity profile. The quadratic fit has the form  $u_t = u_0 \cdot \tilde{r}(1 - \tilde{r})$ . (c) Transport coefficient  $q(t) = V_t/V$ , for three different annulus widths. In the transport state (red line), the ratio remains close to 0.8. This is coherent with the average profiles described in Fig. 1 (d) showing that the radial component of the velocity is negligible. Furthermore, the time dependence is weak compared to the other signals: the ratio typically fluctuates about  $0.82 \pm 0.09$ . In the switching state (green line), this ratio drops significantly, and the fluctuations are larger ( $0.31 \pm 0.22$ ). Sometimes, the transport velocity changes sign, which attests for occasional flow reversals. Finally, in the turbulent state (blue line), the transport is almost negligible, with oscillations about  $0.05 \pm 0.2$ . Note that, in the particular experiment displayed here, a large fluctuation is observed at time  $t = 160\text{s}$ , with the ratio shooting down to  $-0.6$ .

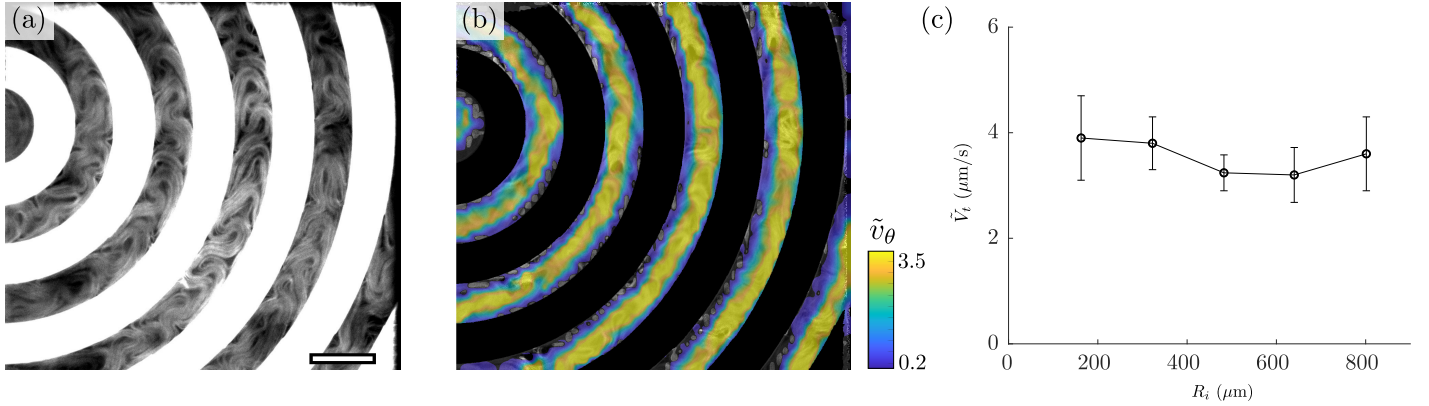


**Fig. S2 Role of the average channel curvature.** (a) Fluorescence micrographs of concentric annuli with the same width,  $60\ \mu\text{m}$ , corresponding to the transport regime, and different inner radius,  $R_i$ . Scale bar:  $100\ \mu\text{m}$ . The image is overlapped with a black mask around the region of interest, for a better visualization. (b) Corresponding intensity maps with the time-averaged absolute value of the azimuthal component of the velocity. Only values above  $0.2\ \mu\text{s}^{-1}$  are represented. (c) Mean azimuthal speed as a function of  $R_i$ .

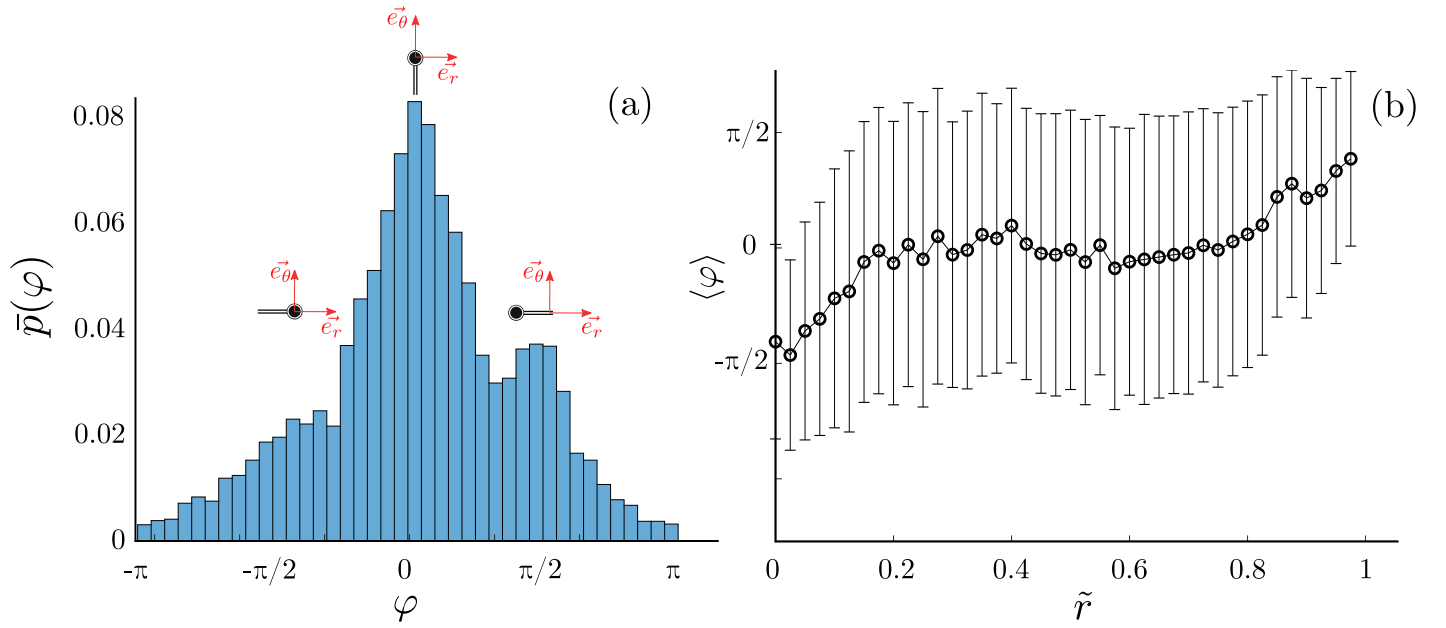


**Fig. S3 Distribution of defect orientations.** Defect positions and orientations are computed with Matlab routines (see Methods). The orientations are then projected onto the azimuthal direction  $\theta$ . Statistics are obtained from a video of 600 frames at 2 frames/s. See Methods section. (a) Distribution of defect orientations in a  $80 \mu\text{m}$  wide annulus. (b) Average defect orientation as a function of the radial coordinate. Error bars correspond to the standard deviation of the measurements.

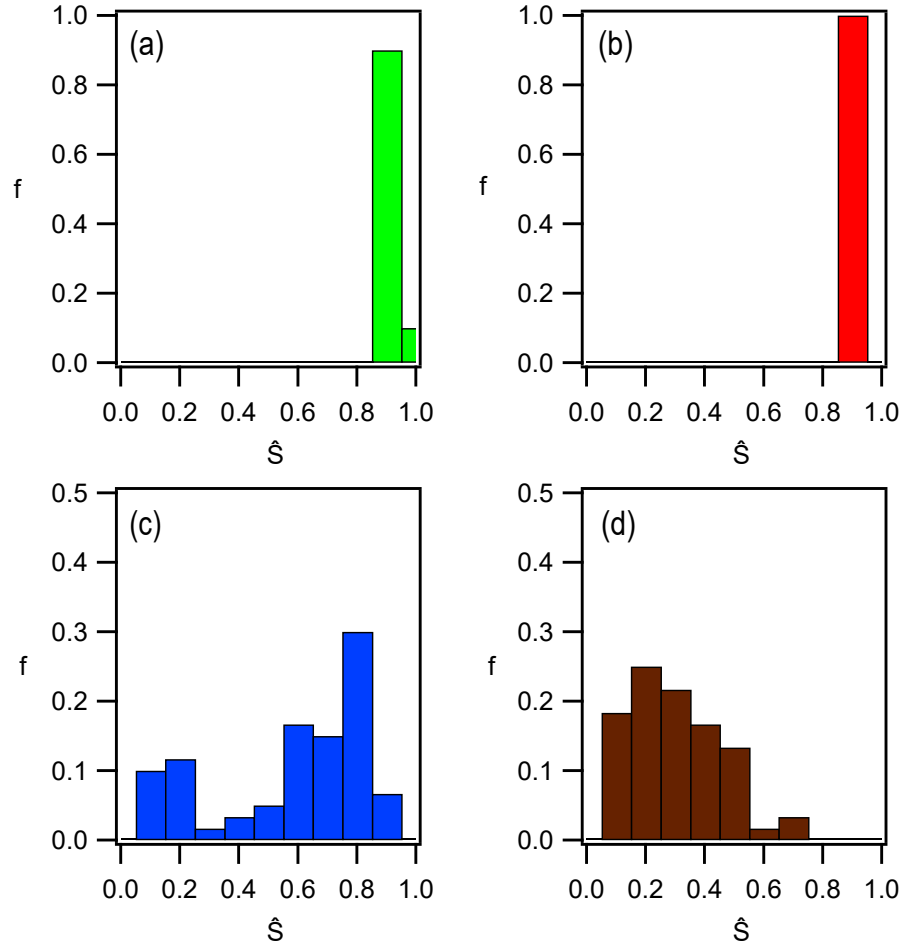


**Fig. S4 Time distribution of the flow order parameter.** Normalized frequency distribution ( $f$ ) of the flow order parameter,  $\hat{S}$ , for active flow in annuli of width 60  $\mu\text{m}$  (a), 80  $\mu\text{m}$  (b), 110  $\mu\text{m}$  (c), and 200  $\mu\text{m}$  (d).



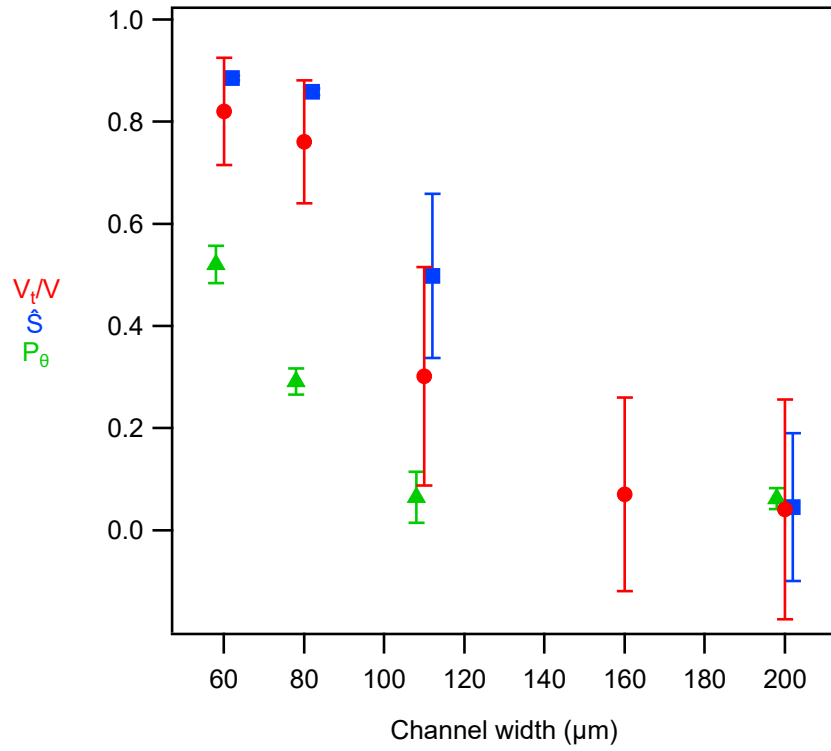


**Fig. S5 Comparison between different order parameters.** Different order parameters of active flows, averaged over time, as a function of the annulus width: tangential velocity,  $V_t$ , divided by the total speed,  $V$  (○); flow order parameter,  $\hat{S}$  (□); defect orientational order parameter,  $P_\theta$  (△).

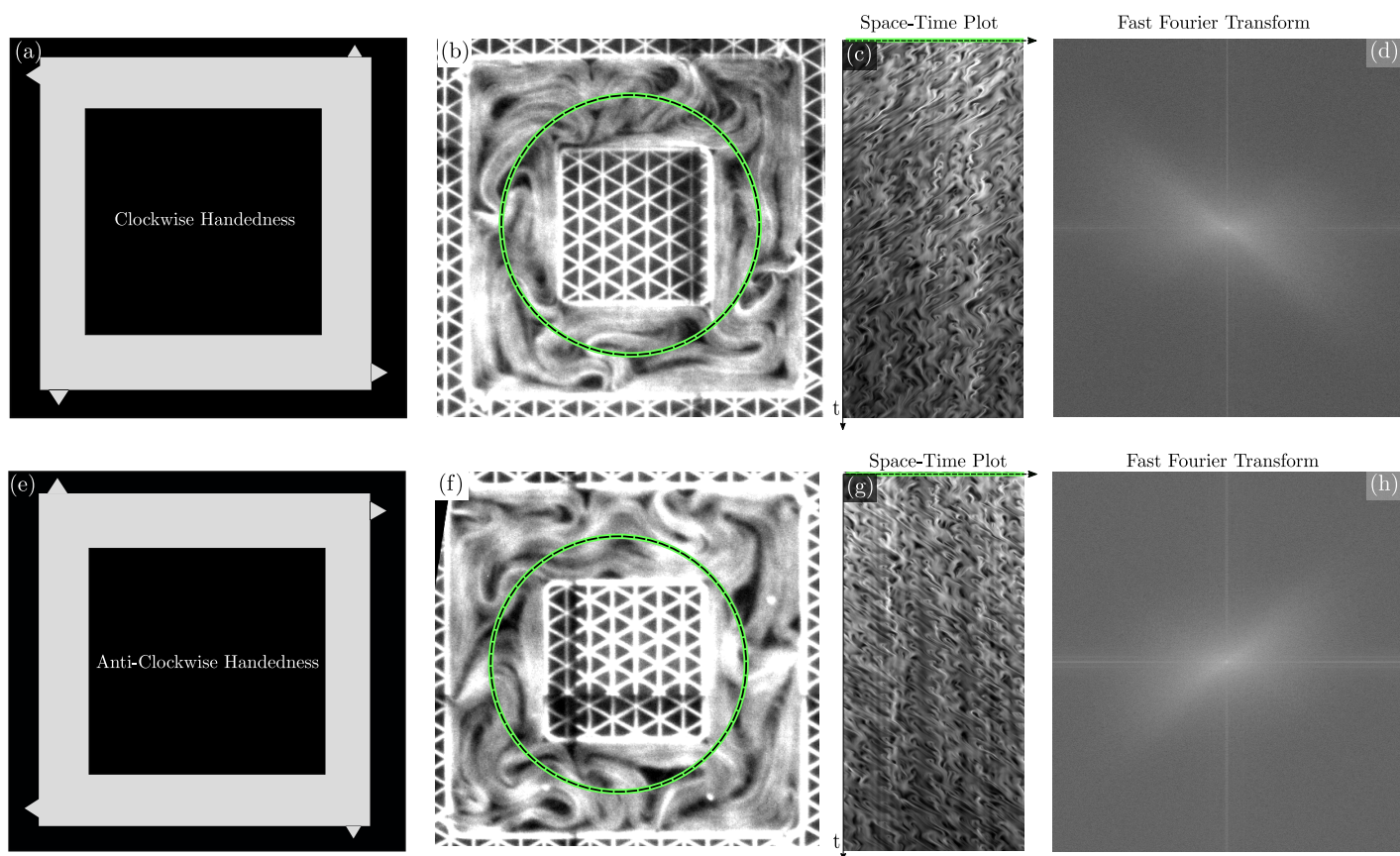
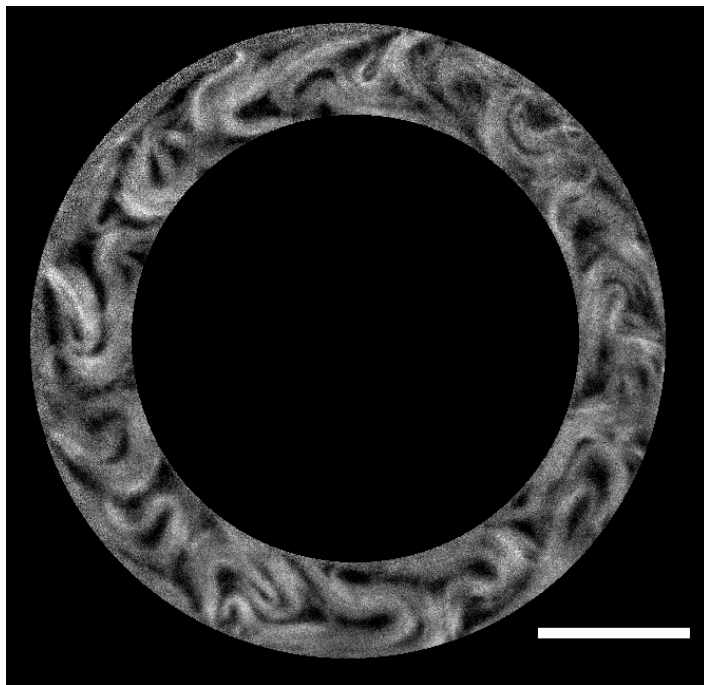
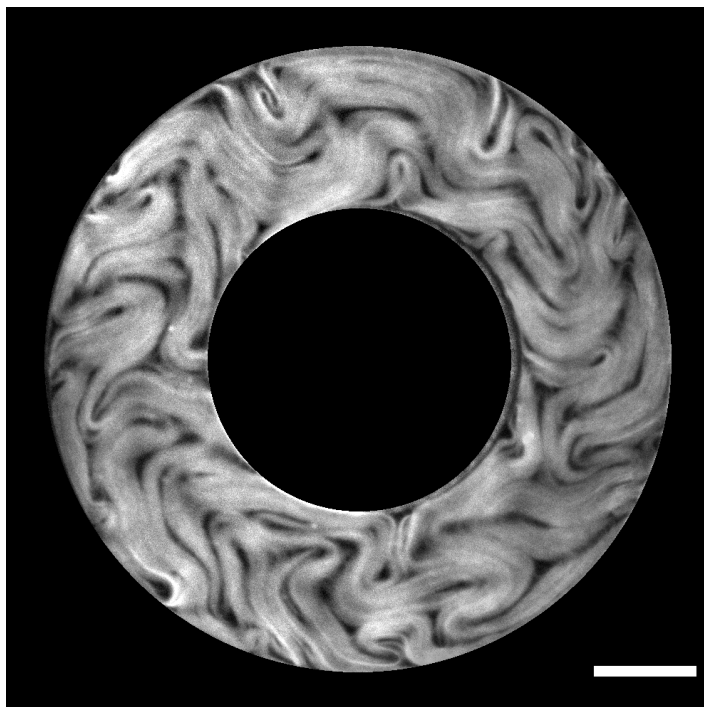


**Fig. S6 Wall-induced rectification in asymmetric annuli.** (a,e) Sketches of square annuli with asymmetric outer boundaries. (b,f) Fluorescence micrographs of active nematics confined in asymmetric square annuli. (e,g) Time-series of a pixel ring at the center of the annuli. (d,h) FFT computation of the times series (e,g) showing clockwise (resp. counter-clockwise) transport.

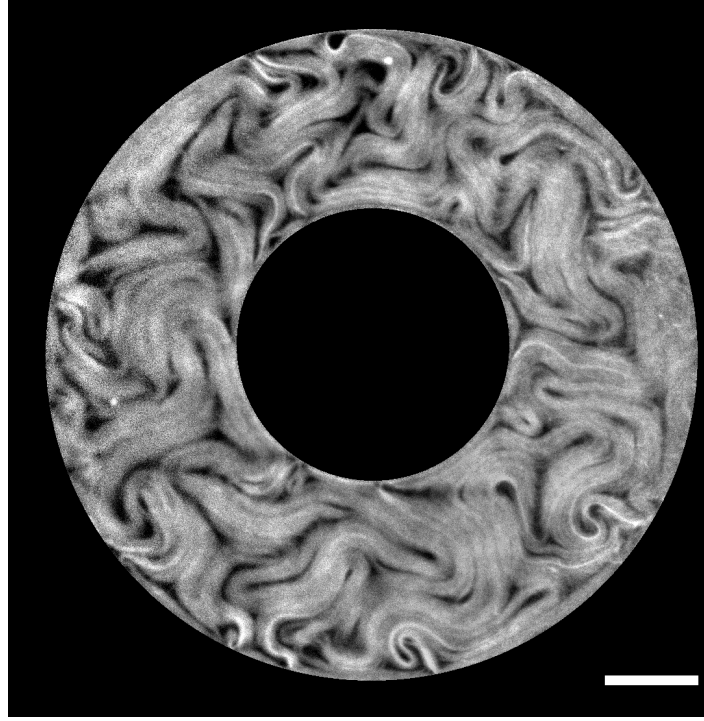
# Supplementary Video Captions



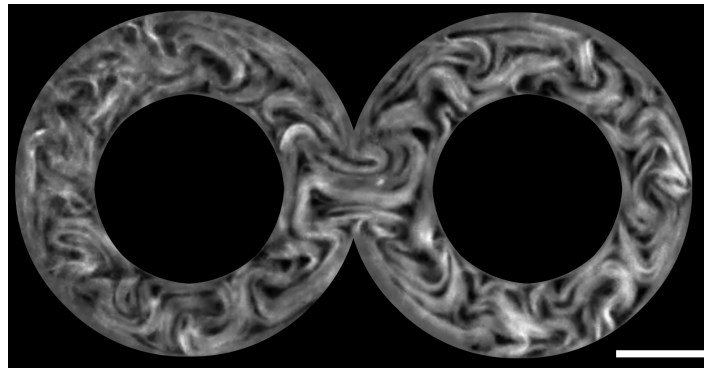
**Movie S1 Symmetry Breaking.** Confocal fluorescence video of active nematics confined in a  $60\ \mu\text{m}$  wide annulus. The image is overlapped with a black mask around the region of interest, for a better visualization. *scale bar:*  $100\ \mu\text{m}$ .



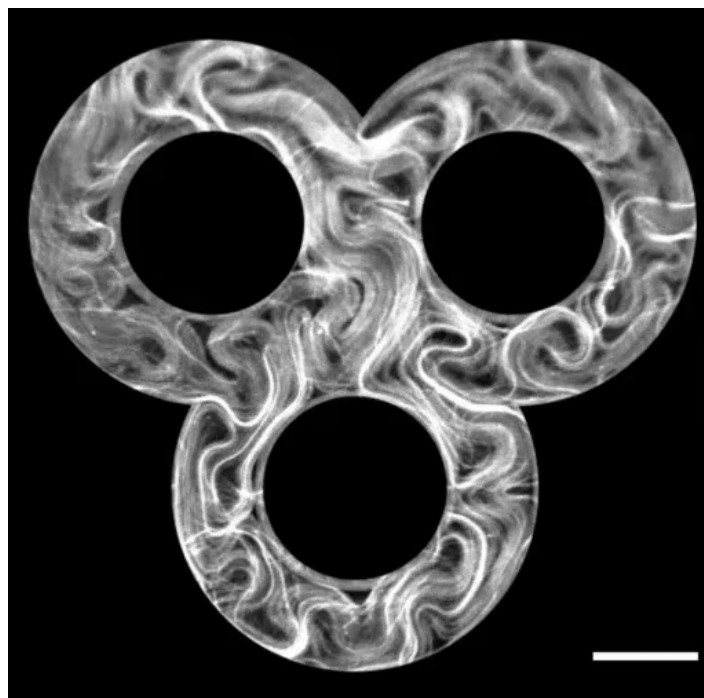
**Movie S2 Switching state.** Confocal fluorescence video of active nematics confined in a  $110\ \mu\text{m}$  wide annulus. The image is overlapped with a black mask around the region of interest, for a better visualization. Scale bar:  $100\ \mu\text{m}$ .



**Movie S3 Turbulent state.** Confocal fluorescence video of active nematics confined in a  $200\ \mu\text{m}$  wide annulus. The image is overlapped with a black mask around the region of interest, for a better visualization. Scale bar:  $100\ \mu\text{m}$ .



**Movie S4 Synchronisation in a Genus 2.** Confocal fluorescence video of active nematics confined in a genus 2 handle-body, with an overlapping distance of  $D/2R_0 = 0.94$ . The width of each annulus is  $w = 80\ \mu\text{m}$ . The image is overlapped with a black mask around the region of interest, for a better visualization. Scale bar:  $100\ \mu\text{m}$ .



**Movie S5 Frustration in a Genus 3.** Confocal fluorescence video of active nematics confined in a genus 3 handle-body. The width of each annulus is  $w = 80 \mu\text{m}$  and the overlapping distance is  $D/2R_0 = 0.83$ . The image is overlapped with a black mask around the region of interest, for a better visualization. Scale bar:  $100 \mu\text{m}$ .